

# Characterization of Multicrystalline Silicon Solar Wafers Fracture Strength and Influencing Factors

V.A. Popovich<sup>1</sup>, A.C. Riemsdag<sup>1</sup>, M. Janssen<sup>1</sup>, I.J. Bennett<sup>2</sup>, I.M. Richardson<sup>1</sup>

Delft University of Technology, Department of Materials Science and Engineering, Delft, The Netherlands<sup>1</sup>;

Energy Research Centre of the Netherlands, Solar Energy, PV Module Technology, Petten, The Netherlands<sup>2</sup>

Email: v.popovich@tudelft.nl

## Abstract

Silicon wafer thickness reduction without increasing the wafer strength leads to a high fracture rate during subsequent handling and processing steps. Cracking of solar cells has also become one of the major sources of solar module failure and rejection. Hence, it is important to evaluate the mechanical strength of silicon solar wafers and factors influencing this. The purpose of this work is to understand the fracture behaviour of multicrystalline silicon wafers and to provide information regarding the bending strength of the wafers. The effects on silicon wafer strength of saw damage and of grain size, grain boundaries and triple junctions are investigated. Also the effects of surface roughness and of the damage layer removal process are considered. Significant changes in fracture strength are found as a result of different silicon wafer crystallinity and surface roughness. It was found that fracture strength of the processed silicon wafer is mainly affected by the following factors: the thickness of the saw-damage layer (cracks length), surface roughness, cracks/defects at the edges and the amount of grain boundaries, serving as potential crack initiation points.

## Keywords

*Silicon Solar Cell; Fracture Strength*

## Introduction

Increases in silicon wafer size in combination with continuous wafer thickness reduction without strengthening the wafer leads to a high breakage rate during subsequent handling and processing steps and results in high costs [Popovich V.A; Brun X.F; Wang P.A]. It is well known, that silicon is a brittle material that is easy to break during the in-line process in which several loads are applied on the wafer surface and edges [Lawn B.R; Chen Po-Ying]. Cracking of silicon solar cells has become one of the major sources of solar module failure and rejection. It is essential for silicon wafers to possess maximum fracture strength as it improves the ability of the thin wafers to survive me-

chanical and thermal loads induced by handling and cell processing. Therefore, it is not only important to investigate the electrical properties of silicon solar wafers and cells, but also the mechanical properties, especially the strength. Compared to single crystalline silicon [Hull R; Luque S], relatively little work has been done to characterize the mechanical properties and fracture behaviour of multicrystalline silicon. Factors influencing strength and the mechanism of fracture have to be understood in order to minimize the fracture rate and to optimize the processing steps.

In this work the fracture strength is measured of silicon wafers by a four-point bending method. Results are statistically evaluated by a Weibull analysis, which provides information on the flaw distribution in the sample. Furthermore, Raman spectroscopy and confocal microscopy are used to further characterise the silicon wafers.

The purpose of this research is to determine the nature and source of the defects (flaws) controlling the fracture of multicrystalline silicon solar wafers and to provide information regarding the bending strength of wafers. The resulting data can be used to enhance production yields, improve cell reliability and establish mechanical criteria that lead to a reduction in cell costs. In this paper several aspects are described that affect mechanical strength, *i.e.* silicon wafer crystal structure, saw damage, and surface roughness.

## Experimental Conditions

### *Material preparation*

Bending tests were performed on rectangular multicrystalline (mc) silicon samples of 10 x 30 mm<sup>2</sup> with a thickness of 200 µm. These samples were laser-cut from neighbouring wafers, using a standard industrial

process, from the middle of one cast block, assuring a relatively low defect density. The edges of all specimens were polished down to a 1  $\mu\text{m}$  finish and carefully examined under optical microscope.

Samples with specific types of crystallinity were prepared in order to investigate the effect of crystallinity features on the mechanical strength of the silicon wafer. In order to statistically evaluate the results, 15 neighbouring specimens (thus featuring the same crystallinity features) were prepared. The specimens were divided into 6 groups according to the crystallinity type in the centre of the specimen, see Figure 1, namely: one big grain, a twin boundary, a grain boundary perpendicular to the loading direction, several grains, a triple junction and many small grains.

To analyze the effect of surface roughness three types of specimens were prepared from neighbouring wafers, thus having the same crystallinity. The surface condition of these specimens included:

- The as-cut state, thus including the saw-damage layer.
- A surface textured by etching 30 s in a HF (10%) + HNO<sub>3</sub> (30%) + CH<sub>3</sub>COOH (60%) solution. This serves two main purposes: to remove the damaged layer and to create a highly textured silicon surface in order to trap the light.
- A chemically polished surface (15  $\mu\text{m}$  removal from both wafer sides in HF+HNO<sub>3</sub> bath for 1 min.).

Confocal microscopy was used to evaluate the obtained surface roughness profiles.

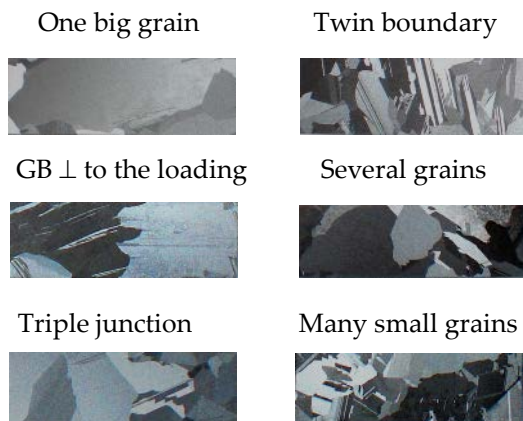


FIGURE 1 GROUPS OF SPECIMENS SHOWING TYPICAL CRYSTALLINITY FEATURES

### Raman spectroscopy

The effects of saw damage removal were analyzed using Raman spectroscopy by comparing results from as-cut wafers with those from etched specimens. In all cases only neighbouring wafers were used. The Raman measurement was carried out at room temperature in the backscattering configuration. A Renishaw Raman spectrometer was used, equipped with a He-Ne laser with an excitation wavelength of 633 nm and a 100 $\times$  objective, resulting in a focused spot with a diameter of  $\sim 1 \mu\text{m}$  and a penetration depth of a few  $\mu\text{m}$  in silicon. The measurement was performed in 3 accumulations with 5% of the total 50 W power. The c-Si TO peak was fitted to a Lorentzian distribution.

Raman spectroscopy gives information on the plane stress state in the outer surface layer (a few  $\mu\text{m}$ ) of the silicon. In the technique used here, in which no polarised light is used, information is obtained on the average in-plane normal stress,  $\sigma$ . This information is contained in the wave number  $\omega$  (inverse of wavelength) of the Raman peak. The value of  $\sigma$  relative to some reference state,  $\Delta\sigma$ , can be evaluated from the shift  $\Delta\omega = \omega_s - \omega_0$ , with  $\omega_0$  being the peak position in the reference state and  $\omega_s$  the peak position of the stressed state. Discarding the effect of grain orientation on this effect, the following approximate relations hold for:

- a uniaxial stress state [Kimoto, K.]:

$$\Delta\sigma \text{ (MPa)} = -500 \Delta\omega \text{ (cm}^{-1}\text{)} \quad (1)$$

- a biaxial state [Wolf de I.]:

$$\Delta\sigma \text{ (MPa)} = -250 \Delta\omega \text{ (cm}^{-1}\text{)} \quad (2)$$

Thus a shift of the Si Raman peak towards lower wave numbers corresponds to tensile stress and vice versa. Note that if a biaxial stress state exists in the wafer, this will be reduced to a uniaxial state by cross-sectioning the wafer.

Considering the experimental resolution of  $\pm 0.1 \text{ cm}^{-1}$ , stresses can be evaluated within  $\pm 20 \text{ MPa}$  [Wolf de I.].

### Strength measurement

The four-point bending test was chosen in this research because this type of loading results in a uniform bending moment along the central part of the specimen. Silicon is a crack-sensitive material and its failure is driven by tension rather than compression. Fracture mechanics predicts that fracture will initiate on the tensile side at the location where the largest surface or edge defect is present. Loading a significant part of the specimen length to uniform tension reduces the spread obtained in the strength results.

To a large extent the test configuration complies with ASTM standard C 1161-02c, which is on the measurement of the flexural strength of ceramic material at ambient temperature. The bending tests were performed using a 100 kN Instron 5500R tensile machine equipped with a 10 N load cell. During the test the load and crosshead displacement were recorded until fracture. The crosshead speed was set such that the outer-fibre strain rate in the specimen was of the order of  $10^{-4} \text{ s}^{-1}$ .

For this research, a new testing fixture was designed especially for the thin silicon specimens taken from wafers. The configuration of the testing fixture is shown in Figure 2. The test fixture had a loading span equal to half the support span (*i.e.* a four-point -  $\frac{1}{4}$  point configuration) and was semi-articulating.

It should be noted, that loading and supporting rollers are fixed  $\varnothing$  1.0 mm cylinders. This deviates from ASTM standard C 1161, which prescribes that:

- The roller diameter should be approximately 1.5 times the specimen thickness. However, such a small diameter would not be very practical in this case.
- During the bending test the loading and supporting rollers should be free to rotate inwards and outwards respectively. The fixed configuration used in this work will inevitably introduce some friction between rollers and specimen.

In order to investigate possible effects of friction, three different types of rollers were considered: as received, polished down to  $1 \mu\text{m}$  and covered with  $300 \mu\text{m}$  thick PTFE foil. However, as a result of our observations, polished rollers were chosen in this research in order to minimize frictional constraints between rollers and specimen surface as much as possible.

The friction occurring at the loading rollers will induce a tensile stress in the central part of the specimen. It can be reasoned, that for the four-point bending configuration the ratio of this friction stress  $\sigma_f$  and the outer-fibre bending stress  $\sigma_b$  is equal to

$$\frac{\sigma_f}{\sigma_b} = \frac{4df}{3L} \quad (3)$$

Where  $d$  = specimen thickness,  $f$  = friction coefficient between roller and specimen and  $L$  = support span. Considering the very low value for  $d/L$  in our set-up (0.0033), the resulting stress ratio will always be very small. Therefore the use of fixed rollers is not expected to affect the results.

Typical 4-point-bending load-displacement curves of silicon samples with different crystallinity features are shown in Figure 3. As can be seen, the curves are almost identical with the exception of the failure loads. They exhibit linear behaviour up to the failure point, so a linear elastic stress distribution is assumed over the specimen thickness. The outer fibre stress  $\sigma$  in a rectangular beam specimen loaded in the 4-point bending configuration used [ASTM standard C 1161-02c] is:

$$\sigma = \frac{3PL}{4bd^2} \quad (4)$$

where  $P$  = applied force and  $b$  = width of the specimen.

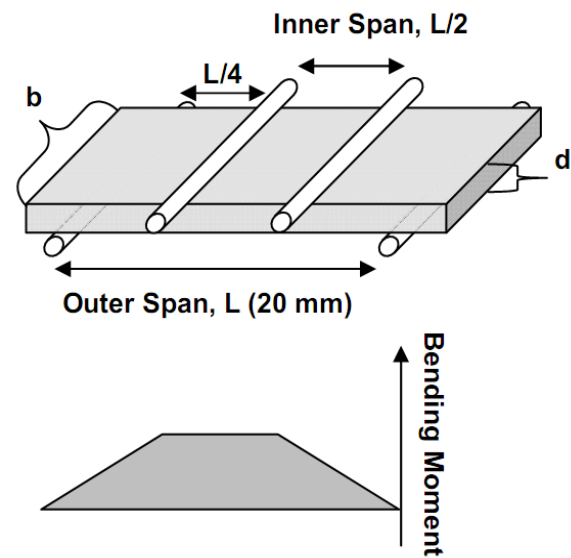


FIGURE 2 ILLUSTRATIONS OF THE FOUR-POINT BENDING TEST SETUP AND A CORRESPONDING BENDING MOMENT DIAGRAM

In order to prevent errors coming from the improper loading, load-displacement curves were closely monitored during the tests.

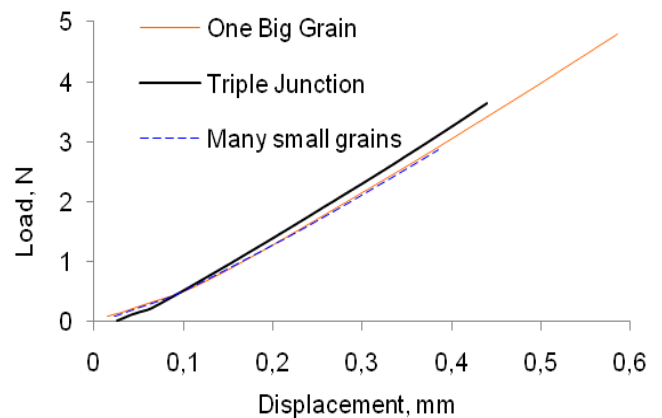


FIGURE 3 REPRESENTATIVE LOAD-DISPLACEMENT CURVES FOR SAMPLES WITH DIFFERENT CRYSTALLINITY

The strength of a brittle material such as silicon is de-

terminated by the presence of defects that lead to crack initiation. A large scatter of the measured strength data will be observed, caused by the random distribution of defect location, size and orientation. Weibull statistics, based on the concept of the weakest link, is applied to describe the probability of failure by using two parameters [ASTM C 1239-95]:

$$P_f = 1 - \exp \left[ - \left( \frac{\sigma}{\sigma_0} \right)^m \right] \quad (5)$$

where  $P_f$  is the probability of failure at an applied tensile stress  $\sigma$ , while  $\sigma_0$  and  $m$  are the characteristic strength and the Weibull modulus of the specimen respectively. The characteristic strength,  $\sigma_0$ , is the tensile stress at which 63.2% of all samples are expected to fail. The Weibull modulus,  $m$ , is a measure for the scatter of the measured strength values around the median strength. A large value stands for little scatter, which can be associated with a narrow defect distribution. Estimates for the Weibull parameters  $\sigma_0$  and  $m$ , are found by making a plot of  $\ln[\ln[1/(1-P_f)]]$  as a function of  $\ln(\sigma)$ . Data for this plot are obtained on the basis of experimental results on a sufficiently high number of similar specimens using the procedure described in [Weibull, W].

## Results and Discussion

### *Effect of saw-damage on mechanical strength*

Silicon specimens were cut using a conventional multi-wire-sawing process in order to see its influence on microstructure and mechanical strength.

Figure 4 represents a schematic illustration of wire saw cutting process. As can be seen, silicon cutting utilizes a steel wire, under high tension, that moves at high speed along the surface of the substrate. The wire is submerged in abrasive slurry, consisting of abrasive grit suspended in carbon fluid [Kao, I.]. When the abrasive particles are big, the damage of the Si surface is large and there are several large, deep grooves across the surface. The region near these grooves contains much damage and residual stresses.

Figure 5 shows a typical surface of an as-cut multicrystalline silicon wafer, containing large amount of smooth grooves. As-cut silicon samples were analyzed with a Raman spectrometer to investigate a nature of smooth grooves and to check for phase transfor-

mations in the damaged surface layer.

The Raman spectrum, shown in figure 6, clearly indicates the presence of amorphous Si (a-Si) next to polycrystalline Si on the as-cut surface. Many points at different positions on the wafer surface have been measured and in many of them a similar a-Si peak was found, either big or small.

As shown in figure 4, the microscopic silicon material removal process can be explained by the interaction of loose, rolling SiC particles that are randomly indented into the silicon surface until small crystal pieces are chipped away. Since SiC particles are faceted and contain sharp edges and tips, they can introduce very high local pressures on the surface [Gassilloud, R.].

It is known that when indented/scratched silicon, it locally induces a high pressure and silicon exhibits a phase transition from cubic diamond (Si-I) into a metallic (ductile)  $\beta$ -tin structure (Si-II). During the fast unloading this ductile phase is not stable and transforms into a layer of amorphous silicon or – if the unloading is slow enough – a mixture of amorphous and metastable phases (Si-XII- rhombohedral structure with 8 atoms per unit cell and Si-III phases *bc8*, body-centred cubic structure with 16 atoms per unit cell) is formed [Jang, J.-I; Kailer, A.].

In our study, the Si phase transition into amorphous silicon phase was found only in the smooth grooves (Figure 5). The rough parts of as-cut silicon wafer surfaces, where material is chipped off, mainly consist of stable crystalline silicon.

In order to see the influence of saw damage on the stress state and the mechanical strength of silicon wafers, 2 types of specimens were mechanically tested: as-cut specimens and specimens etched by an acidic solution to remove the damaged layer. The results, presented in Table 1, show that the as-cut specimens have a lower Weibull characteristic strength,  $\sigma_0$ , which is presumably due to the presence of microcracks at the surface that is loaded in tension.

It is known that wafer strength is directly related to the density and the size of microcracks [Cook, R.F.; Gere, J.M.]. If density and size of microcracks are high, the probability that a macrocrack initiates and leads to failure for a given stress is also high.

Microcracks are induced during the sawing process while slicing the wafers from the ingot, which explains

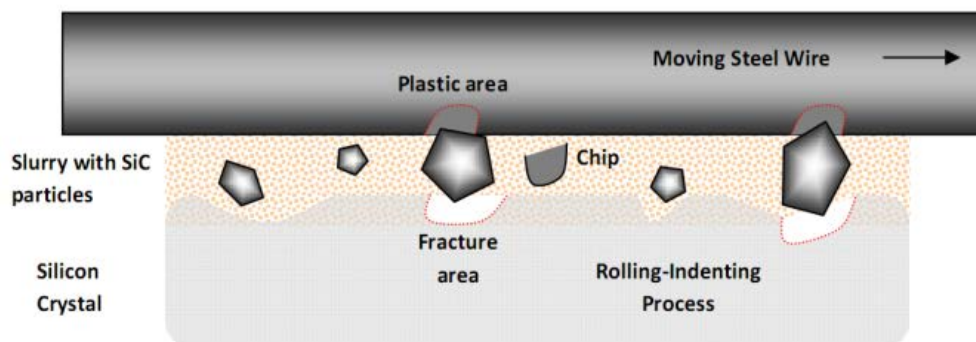


FIGURE 4 SCHEMATIC ILLUSTRATION OF THE ROLLING-INDENTING PROCESS IN THE WIRE-SAWING CUTTING PROCESS IN WHICH THE WIRE INTRODUCES FORCE ON THE ROLLING ABRASIVE SIC PARTICLES, THUS INDENTING THE CONTACT INTERFACE AND REMOVING MATERIALS FROM THE SURFACE

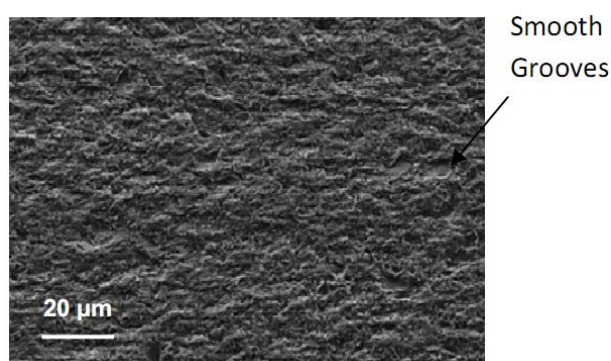


FIGURE 5 SCANNING ELECTRON MICROSCOPY MICROGRAPH OF A TYPICAL SURFACE OF THE AS-CUT MULTICRYSTALLINE SILICON WAFER

the lower strength in specimens in the as-cut state. Additionally, the presence of transformed a-Si phase could possibly also affect mechanical stability of the as-cut wafers.

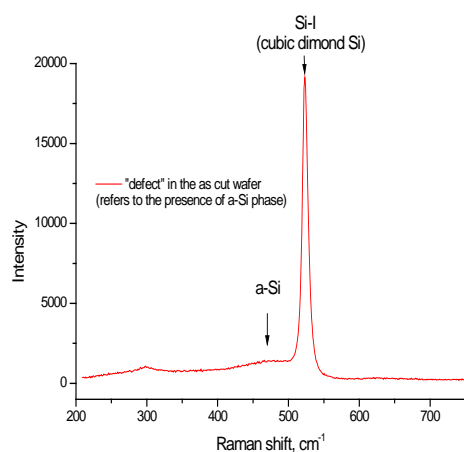


FIGURE 6 REPRESENTATIVE RAMAN SPECTRUM FOR THE AS-CUT WAFER SURFACE, SHOWING LOCAL INDENTATION-INDUCED TRANSFORMATION OF SI INTO AMORPHOUS SI

As a result of the etching process, the depth of surface microcracks is reduced, some cracks disappear com-

pletely and some crack tips become more blunted. Furthermore, the layer of transformed a-Si is removed. All these effects reduce the probability of macrocrack initiation, increasing the specimen strength.

In this work, Raman spectroscopy was also used to characterize the stress state in the damaged layer of the as-cut silicon wafer. As can be seen from Figure 7, there is a significant positive shift of the Raman peak for as-cut samples relative to the damage-free etched samples. This shift,  $\Delta\omega$ , of  $2\text{ cm}^{-1}$  corresponds to a tensile stress of 500 MPa, assuming a biaxial stress state.

TABLE 1 EFFECT OF DAMAGED LAYER ON WEIBULL CHARACTERISTIC STRENGTH ( $\sigma_0$ ) AND MODULUS ( $m$ )

Surface condition	$\sigma_0$ (MPa)	$m$ (-)
as-cut	155	9.4
after etching	234	8.3

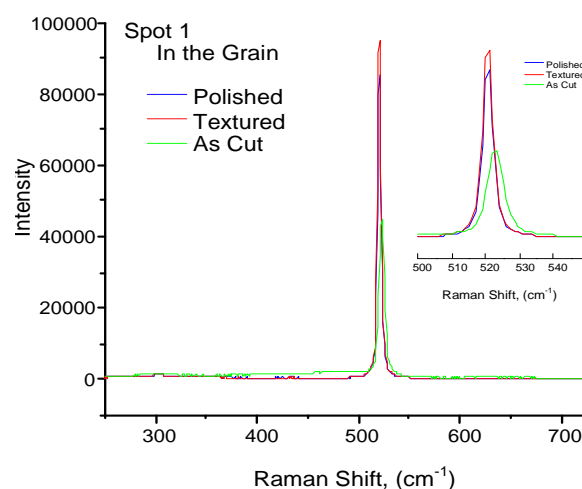


FIGURE 7 REPRESENTATIVE RAMAN SPECTRA OF THE AS-CUT, TEXTURED AND POLISHED NEIGHBOURING WAFERS

This stress value is representative only for the top few microns of the damaged layer, as this is the penetra-



tion depth of Raman Spectroscopy in silicon material.

### ***Effect of surface roughness on mechanical strength***

In this study, the as processed silicon wafers thickness remains the same, and the wafer edges are polished down to 1  $\mu\text{m}$ . Therefore these factors will not influence the strength and the surface roughness completely determines the fracture strength of the multicrystalline silicon wafer specimens.

In order to investigate the effect of surface roughness on strength, three sets of specimens taken from neighbouring wafers (thus featuring the same crystallinity) with different surface conditions were tested, *i.e.* as cut, textured and polished down 15  $\mu\text{m}$ . Figure 8 shows representative confocal microscopy surface roughness profiles, taken after the respective surface treatments in the same areas of the neighbouring samples.

Table 2 contains the determined roughness parameters  $S_z$  and  $S_{dr}$ . As can be seen, samples with a textured surface show a significantly higher surface roughness compared to the as-cut state, presumably due to the formation of etch pits. It should also be noted, that etching/texturing creates a much rougher surface at the grain boundaries, probably due to local preferential etching (etched sample in Figure 8a).

The low value of Weibull modulus for the textured samples ( $m = 8.3$ ; see Table 2) shows that apparently there is much variation in the size of the largest defects present at the tensile surface. However, despite the increase of the surface roughness, there is an increase of 50% in the characteristic strength as a result of the etching/texturing, probably due to the removal of the damaged layer.

Thus, it is suggested, that the size of microcracks in the damaged layer is a more dominant factor affecting mechanical strength of silicon wafers than the surface

roughness.

Polishing the silicon wafers showed the expected reduction in surface roughness, as well as a significant increase in fracture strength (Table 2). A larger Weibull modulus, as compared to the as-cut and the textured state, indicates that the polishing process gives a much smoother silicon surface and a narrower defect distribution.

It can be concluded that, as long as saw-damage is removed, the surface roughness profile is the second most detrimental factor affecting mechanical strength of silicon wafers.

It can also be concluded, that the fracture strength of polished and textured silicon wafers is inversely proportional to the surface roughness, correlated as:  $F_s \sim 1/R_a$ , where  $F_s$  is fracture strength and  $R_a$  is surface roughness profile.

### ***Effect of mc-silicon wafer crystallinity on mechanical strength***

Specific types of silicon wafers crystallinity were chosen for this research to investigate the effect on mechanical strength. All specimens were etched by an acidic solution for 30 s to remove the damaged layer induced by the sawing process. The four-point bending strength was analyzed by Eg. (4). The results are given in Table 3, which lists the Weibull characteristic strength ( $\sigma_\theta$ ) and the Weibull modulus ( $m$ ) of 15 tests.

As can be seen from Table 3, it is possible to define three main characteristic groups, based on the strength results. The specimens with one big grain in the middle have a much higher strength than those with many small grains in the middle. The four other crystallinity types, all having several grains in the middle, have intermediate strengths.

As for most brittle materials, the fracture strength of an

TABLE 2 EFFECT OF SURFACE ROUGHNESS PARAMETERS ON BENDING STRENGTH AND WEIBULL PARAMETERS OF MULTICRYSTALLINE SILICON WAFERS

Silicon Surface Treatment	In the Grain		Grain Boundary		$\sigma_\theta$ (MPa)	$m$ (-)
	$S_z$	$S_{dr}, \%$	$S_z$	$S_{dr}, \%$		
As Cut	5.70	14.6	6.11	12.2	160	9.4
Textured	12.7	28.2	13.7	45.8	240	8.3
Polished	9.73	10.8	10.6	10.0	285	10.1

$S_z$  is an average difference between the 5 highest peaks and 5 lowest valleys;  $S_{dr}$  is the developed Interfacial Area Ratio, which is expressed as the percentage of additional surface area contributed by the texture as compared to an ideal plane the size of the measurement region.

TABLE 3 EFFECT OF CRYSTALLINITY TYPE OF ETCHED WAFERS ON MECHANICAL STRENGTH

Crystallinity type	$\sigma_0$ (MPa)	$m$ (-)
One big grain	287	7.9
Twin boundary	256	8.6
Triple junction	255	5.9
GB perpendicular to the loading direction	241	8.4
Several grains	228	5.5
Many grains	208	5.7

mc-silicon wafer depends on both material-intrinsic properties, such as grain size, grain boundaries and crystal orientation, and on extrinsic variables such as flaws and microcracks [Moller, H.J.].

The strength reduction due to the presence of many small grains might be related to the number of grain boundaries, which is proportional to the number of grains. Alternatively the surface roughness might be different for different crystallinity types, due to preferential etching of the grain boundaries. Surface roughness parameters of the three main crystallinity groups are given in Figure 9. As can be seen, there again seems to be a correlation between surface roughness and the fracture strength: the higher the surface roughness, the lower the fracture strength, Figure 9c.

In order to eliminate the effect of surface roughness, samples with crystallinity features similar to those shown in Figure 1 were polished to further reduce the surface roughness. As can be seen from Table 4, polishing the samples, leads to higher Weibull characteristic strengths and moduli, probably due to a reduction of the roughness at the grain boundaries.

TABLE 4 EFFECT OF CRYSTALLINITY TYPE OF POLISHED WAFERS ON MECHANICAL STRENGTH

Crystallinity type	$\sigma_0$ (MPa)	$m$ (-)
One big grain	293	8.5
Twin boundary	274	8.9
Triple junction	268	6.7
GB perpendicular to the loading direction	266	9.1
Several grains	260	7.4
Many grains	251	6.9

It should be pointed out, that a significant increase of

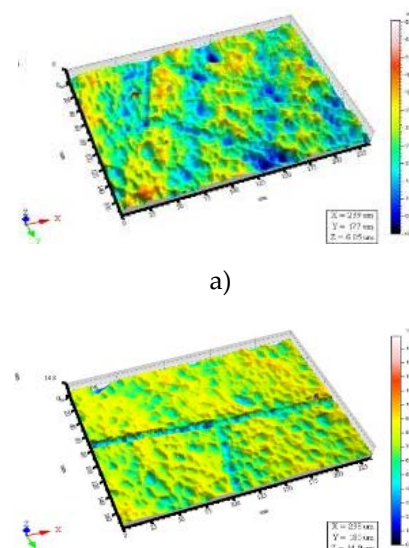
strength is only observed in samples with many grains, which can be related to the levelling off (by the polishing) of etch pits that were formed near the grain boundaries during the texturing/etching process.

Nonetheless, samples with polished surfaces show the same correlation between crystallinity and fracture strength, namely, the higher the number of grain boundaries the weaker the sample is. Furthermore, fracture patterns of the polished silicon samples subjected to 4-point bending revealed a preferential propagation of the cracks along the grain boundaries (Figure 10).

It should be pointed out, that a significant increase of strength is only observed in samples with many grains, which can be related to the levelling off (by the polishing) of etch pits that were formed near the grain boundaries during the texturing/etching process.

Nonetheless, samples with polished surfaces show the same correlation between crystallinity and fracture strength, namely, the higher the number of grain boundaries the weaker the sample is. Furthermore, fracture patterns of the polished silicon samples subjected to 4-point bending revealed a preferential propagation of the cracks along the grain boundaries (Figure 10).

From these results it can be concluded, that for polished silicon wafers crystallinity is the most significant factor affecting the strength, probably due to a lower strength of grain boundaries leading to intergranular fracture of the polished multicrystalline silicon samples. On the other hand, there is a mixed type fracture (transgranular and intergranular) for textured and as-cut silicon wafers, where surface roughness and a damaged surface layer are the most detrimental factors.



b)

Crystallinity type	$S_z$ ( $\mu\text{m}$ )	Sdr (%)	$\sigma_0$ (MPa)
One big grain	7.5	5	287
Triple junction	13	25	255
Many small grains	11	27	208

c)

FIGURE 9 REPRESENTATIVE SURFACE ROUGHNESS PROFILES OF ETCHED SAMPLES: A) ONE BIG GRAIN, B) TRIPLE JUNCTION AND C) SURFACE ROUGHNESS PARAMETERS AND CHARACTERISTIC STRENGTHS

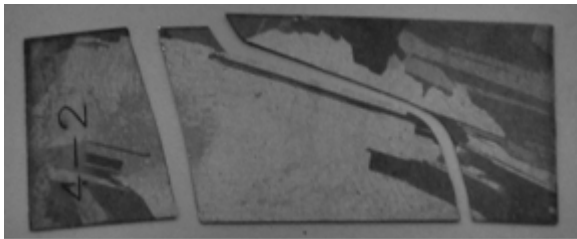


FIGURE 10 EXAMPLE OF THE FRACTURE PATTERN OF A POLISHED MC-SILICON SAMPLE, SHOWING DEFLECTION OF THE CRACK ALONG THE GRAIN BOUNDARY

## Conclusions

The mechanical strength of multicrystalline (mc) silicon solar wafers was investigated using four-point bending tests.

Raman spectroscopy was used to characterise the wafer surfaces. The study showed that:

- The surface layer damaged by the sawing process contains a mixture of indentation-transformed amorphous silicon and a stable crystalline silicon phase;
- The top few microns of the damaged layer contains tensile stresses in the order of 500 MPa (compared to neighbouring damage-free wafers);
- Damage layer removal by etching increases the strength of the mc-silicon wafer by about 50%;
- Samples with removed damaged layer show an inverse proportionality between the surface roughness profile and the fracture strength;
- Mc-silicon wafer crystallinity has a significant effect on the mechanical strength of polished multicrystalline silicon wafers;
- Surface and edge defects, such as microcracks,

grain boundaries and surface roughness are the most probable sources of mechanical strength degradation; reduction of microcracks leads to an increase of the fracture strength of a mc-silicon wafer;

- Results suggest, that there is a mixed type fracture (transgranular and intergranular) for as-cut and for textured silicon wafers. For polished silicon wafers, however, crystallinity is the most significant factor affecting the strength, suggesting a relative weakness of the grain boundaries, leading to an intergranular fracture mode.
- Further than 15 microns mechanical polishing of silicon wafers could further increase fracture strength and result in a reduction of costs.

## REFERENCES

- ASTM Standard C 1161-02c, Standard Test Method for Flexural Strength of Advanced Ceramics at Ambient Temperature, ASTM International, West Conshohocken, USA, 2008.
- ASTM C 1239-95. Reporting Uniaxial Strength Data and Estimating Weibull Distribution Parameters for Advanced Ceramics, 1995.
- Brun, X.F., Melkote, S.N., Analysis of stresses and breakage of crystalline silicon wafers during handling and transport, *Solar Energy Materials and Solar Cells*, Volume 93, 2009, pp. 1238–1247.
- Chen, Po-Ying, Tsai, Ming-Hsing, Relationship between wafer edge design and its ultimate mechanical strength, *Microelectronic Engineering*, Volume 87, Issue 11, November 2010, pp. 2065–2070
- Cook, R.F., Strength and sharp contact fracture of silicon, *J. Mater. Sci.* **41**, 2006.
- Gassilloud, R., Ballif, C., et. al, Deformation mechanisms of silicon during nanoscratching, *Phys. stat. sol. (a)* 202, No. 15, 2005, pp. 2858–2869.
- Gere, J.M., Goodno, B. J., *Mechanics of Materials*, seventh ed., Cengage Learning, USA, 2009.
- Hull R. *Properties of Crystalline Silicon*, Chapter 3, Structural and Mechanical properties (edited by A. George). IN-SPEC, London, 1999
- Jang, J.-I., Lance, M.J., Indentation-induced phase transformations in silicon: Influences of load, rate and indenter angle on the transformation behaviour. *Acta Mater.* **53**(6),



- 2005, pp. 1759–1770
- Kailer, A., Gogotsi, Y.G., Nickel, K.G., Phase transformations of silicon caused by contact loading. *J. Appl. Phys.* **81**(7), 1997, pp. 3057–3063
- Kao, I., Wei, S., Chiang, F.-P.: Vibration of wiresaw manufacturing processes and wafer surface measurement, NSF Des. Manuf. Grantees Conf., Monterey, 1998, pp. 427–428
- Kimoto, K., Usami, K., Japan. *J. Appl. Phys.* **32**, 1993, pp. 211–213.
- Lawn, B.R., *Fracture of Brittle Solids*, Cambridge University Press, 1993.
- Luque, S. Hegedus, "Handbook of Photovoltaic Science and Engineering", John Wiley & Sons Ltd, West Sussex, England, 2003.
- Moller, H.J., Funke, C., Rinio, M., Scholz, S., Multicrystalline silicon for solar cells, *Thin Solid Films*, Volume **487**, Issues 1-2, International Conference on Polycrystalline Semiconductors- Materials, Technologies, Device Applications, 1 September 2005, pp. 179-187.
- Popovich, V.A., Yunus, Janssen, A., M., Richardson, I.M., Bennett, I.J., Effect of silicon solar cell processing parameters and crystallinity on mechanical strength, *Solar Energy Materials and Solar Cells*, Volume **95**, Issue 1, PVSEC-19, Jeju, Korea, 9-13 November 2009, January 2011, pp. 97-100.
- Wang, P.A., Industrial challenges for thin wafer manufacturing, in: *Proceedings of the Fourth World Conference on Photovoltaic Energy Conversion*, Waikoloa, HI, USA, 2006, pp. 1179–1182.
- Weibull, W., A statistical distribution function of wide applicability, *J. Appl. Mech.* **18**, 1951, pp. 293–297.
- Wolf, I. De, "Micro-Raman spectroscopy to study local mechanical stress in silicon integrated circuits", *Semicond. Sci. Technol.* **11**, 1996, pp. 139-154.